

# EdgeNeXt: Efficiently Amalgamated CNN-Transformer Architecture for Mobile Vision Applications

Muhammad Maaz<sup>1,\*</sup> Abdelrahman Shaker<sup>1,\*</sup> Hisham Cholakkal<sup>1</sup> Salman Khan<sup>1,2</sup>  
 Syed Waqas Zamir<sup>3</sup> Rao Muhammad Anwer<sup>1</sup> Fahad Shahbaz Khan<sup>1</sup>

<sup>1</sup>Mohamed Bin Zayed university of Artificial Intelligence <sup>2</sup>Australian National University

<sup>3</sup>Inception Institute of Artificial Intelligence

## Abstract

In the pursuit of achieving ever-increasing accuracy, large and complex neural networks are usually developed. Such models demand high computational resources and therefore cannot be deployed on edge devices. It is of great interest to build resource-efficient general purpose networks due to their usefulness in several application areas. In this work, we strive to effectively combine the strengths of both CNN and Transformer models and propose a new efficient hybrid architecture EdgeNeXt. Specifically in EdgeNeXt, we introduce split depth-wise transpose attention (SDTA) encoder that splits input tensors into multiple channel groups and utilizes depth-wise convolution along with self-attention across channel dimensions to implicitly increase the receptive field and encode multi-scale features. Our extensive experiments on classification, detection and segmentation tasks, reveal the merits of the proposed approach, outperforming state-of-the-art methods with comparatively lower compute requirements. Our EdgeNeXt model with 1.3M parameters achieves 71.2% top-1 accuracy on ImageNet-1K, outperforming MobileViT with an absolute gain of 2.2% with 28% reduction in FLOPs. Further, our EdgeNeXt model with 5.6M parameters achieves 79.4% top-1 accuracy on ImageNet-1K. The code and models are publicly available at [https://t.ly/\\_Vu9](https://t.ly/_Vu9).

## 1. Introduction

Convolutional neural networks (CNNs) and the recently introduced vision transformers (ViTs) have significantly advanced the state-of-the-art in several mainstream computer vision tasks, including object recognition, detection and segmentation [20, 34]. The general trend is to make the network architectures more deeper and sophisticated in the pursuit of ever-increasing accuracy. While striving for higher

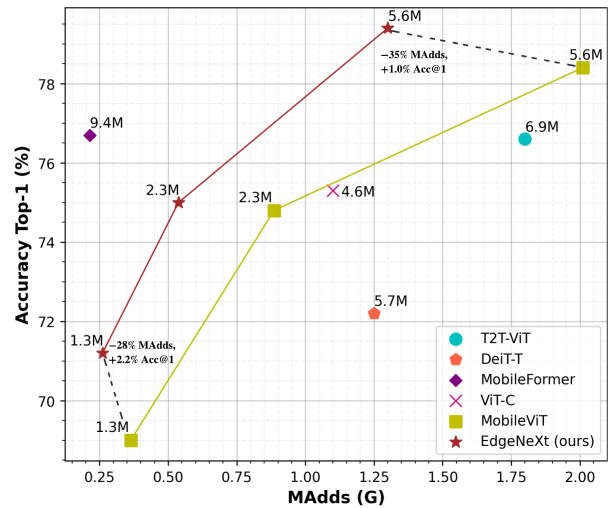


Figure 1. Comparison of our proposed EdgeNeXt models with SOTA ViTs and hybrid architecture designs. The x-axis shows the multiplication-addition (MAdd) operations and y-axis displays the top-1 ImageNet-1K classification accuracy. The number of parameters are mentioned for each corresponding point in the graph. Our EdgeNeXt shows better compute (parameters and MAdds) versus accuracy trade-off compared to recent approaches.

accuracy, most existing CNN and ViT-based architectures ignore the aspect of computational efficiency (*i.e.*, model size and speed) which is crucial to operating on resource-constrained devices such as mobile platforms. In many real-world applications *e.g.*, robotics and self-driving cars, the recognition process is desired to be both accurate and have low latency on resource-constrained mobile platforms.

Most existing approaches typically utilize carefully designed efficient variants of convolutions to achieve a trade-off between speed and accuracy on resource-constrained mobile platforms [19, 28, 33]. Other than these approaches, few existing works [16, 36] employ hardware-aware neural architecture search (NAS) to build low latency accurate

\*Equal contribution

models for mobile devices. While being easy to train and efficient in encoding local image details, these aforementioned light-weight CNNs do not explicitly model global interactions between pixels.

The introduction of self-attention in vision transformers (ViTs) [8] has made it possible to explicitly model this global interaction, however, this typically comes at the cost of slow inference because of the self-attention computation [24]. This becomes an important challenge for designing a lightweight ViT variant for mobile vision applications.

The majority of the existing works employ CNN-based designs in developing efficient models. However, the convolution operation in CNNs inherits two main limitations: First, it has local receptive field and thereby unable to model global context; Second, the learned weights are stationary at inference times, making CNNs inflexible to adapt to the input content. While both of these issues can be alleviated with Transformers, they are typically compute intensive. Few recent works [29, 43] have investigated designing lightweight architectures for mobile vision tasks by combining the strengths of CNNs and ViTs. However, these approaches mainly focus on optimizing the parameters and incur higher multiply-adds (MAdds) operations which restricts high-speed inference on mobile devices. The MAdds are higher since the complexity of the attention block is quadratic with respect to the input size [29]. This becomes further problematic due to multiple attention blocks in the network architecture. Here, we argue that the model size, parameters, and MAdds are all desired to be small with respect to the resource-constrained devices when designing a unified mobile architecture that effectively combines the complementary advantages of CNNs and ViTs (see Fig. 1).

**Contributions.** We propose a new light-weight architecture, named *EdgeNeXt*, that is efficient in terms of model size, parameters *and* MAdds, while being superior in accuracy on mobile vision tasks. Specifically, we introduce split depth-wise transpose attention (SDTA) encoder that effectively learns both local and global representations to address the issue of limited receptive fields in CNNs without increasing the number of parameters and MAdd operations. Our proposed architecture shows favorable performance in terms of both accuracy *and* latency compared to state-of-the-art mobile networks on various tasks including image classification, object detection, and semantic segmentation. Our *EdgeNeXt* backbone with 5.6M parameters and 1.3G MAdds achieves 79.4% top-1 ImageNet-1K classification accuracy which is superior to its recently introduced MobileViT counterpart [29], while requiring 35% less MAdds. For object detection and semantic segmentation tasks, the proposed *EdgeNeXt* achieves higher mAP and mIOU with fewer MAdds and a comparable number of parameters, compared to all the published lightweight models in literature.

## 2. Related Work

In recent years, designing lightweight hardware-efficient convolutional neural networks for mobile vision tasks has been well studied in literature. The current methods focus on designing efficient versions of convolutions for low-powered edge devices [17, 19]. Among these methods, MobileNet [17] is the most widely used architecture which employs depth-wise separable convolutions [5]. On the other hand, ShuffleNet [44] uses channel shuffling and low-cost group convolutions. MobileNetV2 [33] introduces inverted residual block with linear bottleneck, achieving promising performance on various vision tasks. ESPNetv2 [30] utilizes depth-wise dilated convolutions to increase the receptive field of the network without increasing the network complexity. The hardware-aware neural architecture search (NAS) has also been explored to find a better trade-off between speed and accuracy on mobile devices [16, 36]. Although these CNNs are faster to train and infer on mobile devices, they lack global interaction between pixels which limits their accuracy.

Recently, Desovitskiy *et al.* [8] introduces a vision transformer architecture based on the self-attention mechanism [38] for vision tasks. Their proposed architecture utilizes large-scale pre-training data (e.g. JFT-300M), extensive data augmentations, and a longer training schedule to achieve competitive performance. Later, DeiT [37] proposes to integrate distillation token in this architecture and only employ training on ImageNet-1K [32] dataset. Since then, several variants of ViTs and hybrid architectures are proposed in the literature, adding image-specific inductive bias to ViTs for obtaining improved performance on different vision tasks [9, 11, 35, 39, 45].

ViT models achieve competitive results for several visual recognition tasks [8, 24]. However, it is difficult to deploy these models on resource-constrained edge devices because of the high computational cost of the multi-headed self-attention (MHA). There has been recent work on designing lightweight hybrid networks for mobile vision tasks that combine the advantages of CNNs and transformers. MobileFormer [4] employs parallel branches of MobileNetV2 [33] and ViTs [8] with a bridge connecting both branches for local-global interaction. Mehta *et al.* [29] consider transformers as convolution and propose a MobileViT block for local-global image context fusion. Their approach achieves superior performance on image classification surpassing previous light-weight CNNs and ViTs using a similar parameter budget.

Although MobileViT [29] mainly focuses on optimizing parameters and latency, MHA is still the main efficiency bottleneck in this model, especially for the number of MAdds and the inference time on edge devices. The complexity of MHA in MobileViT is quadratic with respect to the input size, which is the main efficiency bottleneck

given their existing nine attention blocks in MobileViT-S model. In this work, we strive to design a new light-weight architecture for mobile devices that is efficient in terms of both parameters and MAdds, while being superior in accuracy on mobile vision tasks. Our proposed architecture, EdgeNeXt, is built on the recently introduced CNN method, ConvNeXt [25], which modernizes the ResNet [14] architecture following the ViT design choices. Within our EdgeNeXt, we introduce an SDTA block that combines depth-wise convolutions with adaptive kernel sizes along with transpose attention in an efficient manner, obtaining an optimal accuracy-speed trade-off.

### 3. EdgeNeXt

The main objective of this work is to develop a lightweight hybrid design that effectively fuses the merits of ViTs and CNNs for low-powered edge devices. The computational overhead in ViTs (e.g., MobileViT [29]) is mainly due to the self-attention operation. In contrast to MobileViT, the attention block in our model has linear complexity with respect to the input spatial dimension of  $\mathcal{O}(Nd^2)$ , where  $N$  is the number of patches, and  $d$  is the feature/channel dimension. The self-attention operation in our model is applied across channel dimensions instead of the spatial dimension. Furthermore, we demonstrate that with a much lower number of attention blocks (3 versus 9 in MobileViT), we can surpass their performance mark. In this way, the proposed framework can model global representations with a limited number of MAdds which is a fundamental criterion to ensure low-latency inference on edge devices. To motivate our proposed architecture, we present two desirable properties.

**a) Encoding the global information efficiently.** The intrinsic characteristic of self-attention to learn global representations is crucial for vision tasks. To inherit this advantage efficiently, we use cross-covariance attention to incorporate the attention operation across the feature channel dimension instead of the spatial dimension within a relatively small number of network blocks. This reduces the complexity of the original self-attention operation from quadratic to linear in terms of number of tokens and implicitly encodes the global information effectively.

**b) Adaptive kernel sizes.** Large-kernel convolutions are known to be computationally expensive since the number of parameters and FLOPs quadratically increases as the kernel size grows. Although a larger kernel size is helpful to increase the receptive field, using such large kernels across the whole network hierarchy is expensive and sub-optimal. We propose an adaptive kernel sizes mechanism to reduce this complexity and capture different levels of features in the network. Inspired by the hierarchy of the CNNs, we use smaller kernels at the early stages, while larger kernels

at the latter stages in the convolution encoder blocks. This design choice is optimal as early stages in CNN usually capture low-level features and smaller kernels are suitable for this purpose. However, in later stages of the network, large convolutional kernels are required to capture high-level features [42]. We explain our architectural details next.

**Overall Architecture.** Fig. 2 illustrates an overview of the proposed EdgeNeXt architecture. The main ingredients are two-fold: **(1)** adaptive  $N \times N$  Conv. encoder, and **(2)** split depth-wise transpose attention (SDTA) encoder. Our EdgeNeXt architecture builds on the design principles of ConvNeXt [25] and extracts hierarchical features at four different scales across the four stages. The input image of size  $H \times W \times 3$  is passed through a patchify stem layer at the beginning of the network, implemented using a  $4 \times 4$  non-overlapping convolution followed by a layer norm, which results in  $\frac{H}{4} \times \frac{W}{4} \times C1$  feature maps. Then, the output is passed to  $3 \times 3$  Conv. encoder to extract local features. The second stage begins with a downsampling layer implemented using  $2 \times 2$  strided convolution that reduces the spatial sizes by half and increases the channels, resulting in  $\frac{H}{8} \times \frac{W}{8} \times C2$  feature maps, followed by two consecutive  $5 \times 5$  Conv. encoders. Positional Encoding (PE) is also added before the SDTA block in the second stage only. We observe that PE is sensitive for dense prediction tasks (e.g., object detection and segmentation) as well as adding it in all stages increases the latency of the network. Hence, we add it only once in the network to encode the spatial location information. The output feature maps are further passed to the third and fourth stages, to generate  $\frac{H}{16} \times \frac{W}{16} \times C3$  and  $\frac{H}{32} \times \frac{W}{32} \times C4$  dimensional features, respectively.

**Convolution Encoder.** This block consists of depth-wise separable convolution with adaptive kernel sizes. We can define it by two separate layers: **(1)** depth-wise convolution with adaptive  $N \times N$  kernels. We use  $k = 3, 5, 7,$  and  $9$  for stages 1, 2, 3, and 4, respectively. Then, **(2)** two point-wise convolution layers are used to enrich the local representation alongside standard Layer Normalization [2] (LN) and Gaussian Error Linear Unit [15] (GELU) activation for non-linear feature mapping. Finally, a skip connection is added to make information flow across the network hierarchy. This block is similar to the ConvNeXt block but the kernel sizes are dynamic and vary depending on the stage. We observe that adaptive kernel sizes in Conv. encoder perform better compared to static kernel sizes (Table 7). The Conv. encoder can be represented as follows:

$$\mathbf{x}_{i+1} = \mathbf{x}_i + \text{Linear}_G(\text{Linear}(\text{LN}(Dw(\mathbf{x}_i)))), \quad (1)$$

where  $\mathbf{x}_i$  denotes the input feature maps of shape  $H \times W \times C$ ,  $\text{Linear}_G$  is a point-wise convolution layer followed by GELU,  $Dw$  is  $k \times k$  depth-wise convolution,  $\text{LN}$  is a normalization layer, and  $\mathbf{x}_{i+1}$  denotes the output feature

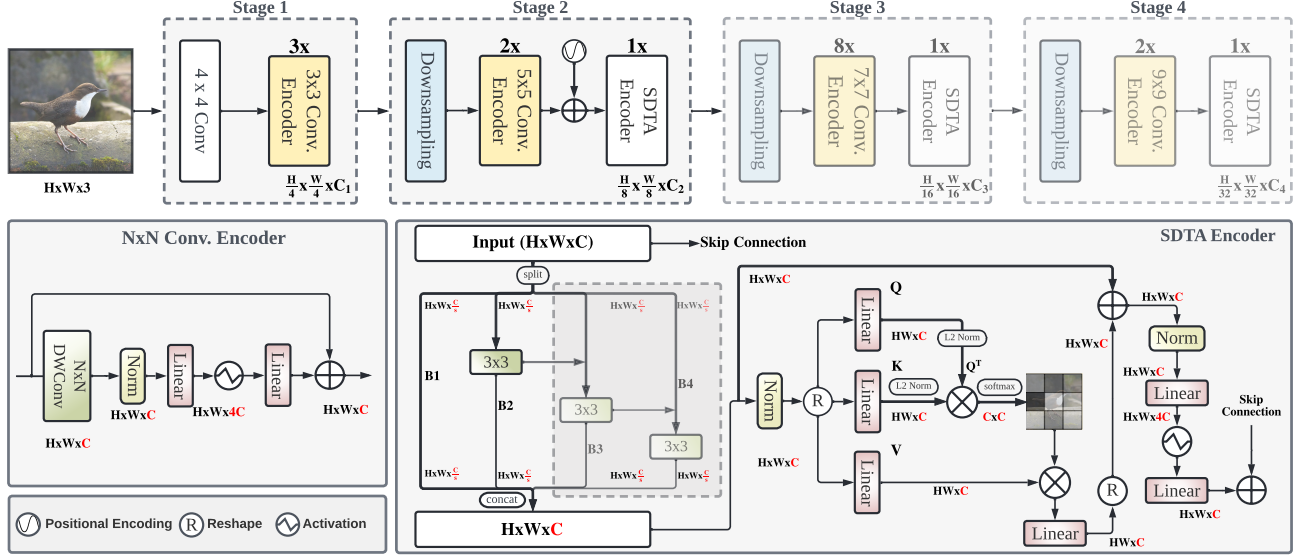


Figure 2. **Top Row:** The overall architecture of our framework is a stage-wise design. Here, the first stage downsamples the input image to  $1/4^{th}$  resolution using  $4 \times 4$  strided convolution followed by three  $3 \times 3$  Convolution (Conv.) encoders. In stages 2-4,  $2 \times 2$  strided convolutions are used for downsampling at the start, followed by  $N \times N$  Convolution and the Split depth-wise Transpose Attention (SDTA) encoders. **Bottom Row:** We present the design of the Conv. encoder (Left) and the SDTA encoder (right). The Conv. encoder uses  $N \times N$  depth-wise convolutions for spatial mixing followed by two pointwise convolutions for channel mixing. The SDTA Encoder splits the input tensor into  $B$  channel groups and applies  $3 \times 3$  depth-wise convolutions for multi-scale spatial mixing. The skip connections between branches increase the overall receptive field of the network. The branches  $B3$  and  $B4$  are progressively activated in stages 3 and 4, increasing the overall receptive field in the deeper layers of the network. Within the proposed SDTA, we utilize Transpose Attention followed by a light-weight MLP, that applies attention to feature channels and has linear complexity with respect to the input image.

maps of the Conv. encoder.

**SDTA Encoder.** There are two main components in the proposed split depth-wise transpose attention (SDTA) encoder. The first component strives to learn an adaptive multi-scale feature representation by encoding various spatial levels within the input image and the second part implicitly encodes global image representations. The first part of our encoder is inspired by Res2Net [12] where we adopt a multi-scale processing approach by developing hierarchical representation into a single block. This makes the spatial receptive field of the output feature representation more flexible and adaptive. Different from Res2Net, the first block in our SDTA encoder does not use the  $1 \times 1$  pointwise convolution layers to ensure a lightweight network with a constrained number of parameters and MAdds. Also, we use adaptive number of subsets per stage to allow effective and flexible feature encoding. In our SDTA encoder, we split the input tensor  $H \times W \times C$  into  $s$  subsets, each subset is denoted by  $\mathbf{x}_i$  and has the same spatial size with  $C/s$  channels, where  $i \in \{1, 2, \dots, s\}$  and  $C$  is the number of channels. Each feature maps subset (except the first subset) is passed to  $3 \times 3$  depth-wise convolution, denoted by  $d_i$ , and the output is denoted by  $\mathbf{y}_i$ . Also, the output of  $d_{i-1}$ , denoted by  $\mathbf{y}_{i-1}$ , is added to the feature subset  $\mathbf{x}_i$ , and then fed into  $d_i$ . The number of subsets  $s$  is adaptive based on the stage number  $t$ , where  $t \in \{2, 3, 4\}$ . We can write  $\mathbf{y}_i$  as

follows:

$$\mathbf{y}_i = \begin{cases} \mathbf{x}_i & i = 1; \\ d_i(\mathbf{x}_i) & i = 2, t = 2; \\ d_i(\mathbf{x}_i + \mathbf{y}_{i-1}) & 2 < i \leq s, t. \end{cases} \quad (2)$$

Each depth-wise operation  $d_i$ , as shown in SDTA encoder in Fig. 2, receives feature maps output from all previous splits  $\{\mathbf{x}_j, j \leq i\}$ .

As mentioned earlier, the overhead of the transformer self-attention layer is infeasible for vision tasks on edge-devices because it comes at the cost of higher MAdds and latency. To alleviate this issue and encode the global context efficiently, we use transposed query and key attention feature maps in our SDTA encoder [1]. This operation has a linear complexity by applying the dot-product operation of the MSA across channel dimensions instead of the spatial dimension, which allows us to compute cross-covariance across channels to generate attention feature maps that have implicit knowledge about the global representations. Given a normalized tensor  $\mathbf{Y}$  of shape  $H \times W \times C$ , we compute query ( $\mathbf{Q}$ ), key ( $\mathbf{K}$ ), and value ( $\mathbf{V}$ ) projections using three linear layers, yielding  $\mathbf{Q} = \mathbf{W}^Q \mathbf{Y}$ ,  $\mathbf{K} = \mathbf{W}^K \mathbf{Y}$ , and  $\mathbf{V} = \mathbf{W}^V \mathbf{Y}$ , with dimensions  $HW \times C$ , where  $\mathbf{W}^Q, \mathbf{W}^K$ , and  $\mathbf{W}^V$  are the projection weights for  $\mathbf{Q}$ ,  $\mathbf{K}$ , and  $\mathbf{V}$  respectively. Then, L2 norm is applied to  $\mathbf{Q}$  and  $\mathbf{K}$  before computing the cross-covariance attention as it stabilizes the

Layer	Output Size	#Layers ( $n$ )	Kernel	Output Channels		
				XXS	XS	S
Image	256×256	1	-	-	-	-
Stem	64×64	1	4×4	24	32	48
Conv. Encoder	64×64	3	3×3	24	32	48
Downsampling	32×32	1	2×2	48	64	96
Conv. Encoder	32×32	2	5×5	48	64	96
STDA Encoder	32×32	1	-	48	64	96
Downsampling	16×16	1	2×2	88	100	160
Conv. Encoder	16×16	8	7×7	88	100	160
STDA Encoder	16×16	1	-	88	100	160
Downsampling	8×8	1	2×2	168	192	304
Conv. Encoder	8×8	2	9×9	168	192	304
STDA Encoder	8×8	1	-	168	192	304
Global Average Pooling	1×1	1	-	-	-	-
Linear	1×1	1	-	1000	1000	1000
<b>Model MAdds</b>				0.3G	0.5G	1.3G
<b>Model Parameters</b>				1.3M	2.3M	5.6M

Table 1. **EdgeNeXt Architectures.** Description of the models’ layers with respect to output size, kernel size, and output channels, repeated  $n$  times, along with the models MAdds and parameters. The number of the output channels for small, extra-small, and extra-extra small models is chosen to match the number of parameters with the counterpart MobileViT model. We use adaptive kernel sizes in Conv. Encoder to reduce the model complexity and capture different levels of features. Also, we pad the output size of the last stage to be able to apply the 9×9 filter.

training. Instead of applying the dot-product between  $\mathbf{Q}$  and  $\mathbf{K}^T$  along the spatial dimension i.e.,  $(HW \times C) \cdot (C \times HW)$ , we apply the dot-product across the channel dimensions between  $\mathbf{Q}^T$  and  $\mathbf{K}$  i.e.,  $(C \times HW) \cdot (HW \times C)$ , producing  $C \times C$  softmax scaled attention score matrix. To get the final attention maps, we multiply the scores by  $\mathbf{V}$  and sum them up. The transposed attention operation can be expressed as follows:

$$\hat{\mathbf{X}} = \text{Attention}(\mathbf{Q}, \mathbf{K}, \mathbf{V}) + \mathbf{X}, \quad (3)$$

$$\text{s.t.}, \text{Attention}(\mathbf{Q}, \mathbf{K}, \mathbf{V}) = \mathbf{V} \cdot \text{softmax}(\mathbf{Q}^T \cdot \mathbf{K})$$

where  $\mathbf{X}$  is the input and  $\hat{\mathbf{X}}$  is the output feature tensor. After that, two 1×1 pointwise convolution layers, LN and GELU activation are used to generate non-linear features. Table 1 shows the sequence of Conv. and STDA encoders with the corresponding input size at each layer with more design details about extra-extra small, extra-small and small models.

## 4. Experiments

In this section, we evaluate our EdgeNeXt model on ImageNet-1K classification, COCO object detection, and Pascal VOC segmentation benchmarks.

### 4.1. Dataset

We use ImageNet-1K [32] dataset in all classification experiments. The dataset provides approximately 1.28M training and 50K validation images for 1000 categories.

Following the literature [17, 29], we report top-1 accuracy on the validation set for all experiments. For object detection, we use COCO [22] dataset which provides approximately 118k training and 5k validation images respectively. For segmentation, we use Pascal VOC 2012 dataset [10] which provides almost 10k images with semantic segmentation masks. Following the standard practice as in [29], we use extra data and annotations from [22] and [13] as well.

### 4.2. Implementation Details

We train our EdgeNeXt models at an input resolution of 256×256 with an effective batch size of 4096. All the experiments are run for 300 epochs with AdamW [27] optimizer, and with a learning rate and weight decay of 6e-3 and 0.05 respectively. We use cosine learning rate schedule [26] with linear warmup for 20 epochs. The data augmentations used during training are Random Resized Crop (RRC), Horizontal Flip, and RandAugment [6], where RandAugment is only used for the EdgeNeXt-S model. We also use multi-scale sampler [29] during training. Further stochastic depth [18] with a rate of 0.1 is used for EdgeNeXt-S model only. We use EMA [31] with a momentum of 0.9995 during training. For inference, the images are resized to 292×292 followed by a center crop at 256×256 resolution. We also train and report the accuracy of our EdgeNeXt-S model at 224×224 resolution for a fair comparison with previous methods. The classification experiments are run on eight A100 GPUs with an average training time of almost 30 hours for the EdgeNeXt-S model.

Frameworks	Models	Date	Input	Params↓	MAdds↓	Top1↑
ConvNets	MobileNetV2	CVPR2018	224 <sup>2</sup>	6.9M	585M	74.7
	ShuffleNetV2	ECCV2018	224 <sup>2</sup>	5.5M	597M	74.5
	MobileNetV3	ICCV2019	224 <sup>2</sup>	5.4M	219M	75.2
ViTs	T2T-ViT	ICCV2021	224 <sup>2</sup>	6.9M	1.80G	76.5
	DeiT-T	ICML2021	224 <sup>2</sup>	5.7M	1.25G	72.2
Hybrid	MobileFormer	CoRR2021	224 <sup>2</sup>	9.4M	214M	76.7
	ViT-C	NeurIPS2021	224 <sup>2</sup>	4.6M	1.10G	75.3
	Coat-Lite-T	ICCV2021	224 <sup>2</sup>	5.7M	1.60G	77.5
	MobileViT-S	ICLR2022	256 <sup>2</sup>	5.6M	2.01G	78.4
	EdgeNeXt-S	Ours	224 <sup>2</sup>	5.6M	965M	78.8
	EdgeNeXt-S	Ours	256 <sup>2</sup>	5.6M	1.30G	79.4

Table 2. Classification performance comparison of our proposed EdgeNeXt model with state-of-the-art lightweight fully convolutional, transformer-based, and hybrid models on the ImageNet-1K validation set. Our model outperforms the SOTA models and achieves a better trade-off between accuracy and compute (i.e., parameters and multiplication-addition (MAdds) operations).

For detection and segmentation tasks, we finetune EdgeNeXt following similar settings as in [29] and report mean average precision (mAP) at IOU of 0.50-0.95 and mean intersection over union (mIOU) respectively. The experiments are run on four A100 GPUs with an average training time of  $\sim 36$  and  $\sim 7$  hours for detection and segmentation respectively.

We also report the latency of our models on NVIDIA Jetson Nano<sup>1</sup> and NVIDIA A100 40GB GPU. For Jetson Nano, we convert all the models to TensorRT<sup>2</sup> engines and perform inference in FP16 mode using a batch size of 1. For A100, similar to [25], we use PyTorch v1.8.1 with a batch size of 256 to measure the latency.

### 4.3. Image Classification

Table 2 compares our proposed EdgeNeXt model with previous state-of-the-art fully convolutional (ConvNets), transformer-based (ViTs) and hybrid models. Overall, our model demonstrates better accuracy versus compute (parameters and MAdds) trade-off compared to all three categories of methods (see Fig. 1).

**Comparison with ConvNets.** EdgeNeXt surpasses lightweight ConvNets by a formidable margin in terms of top-1 accuracy with similar parameters (Table 2). Normally, ConvNets have less MAdds compared to transformer and hybrid models because of no attention computation, however, they lack the global receptive field. For instance, EdgeNeXt-S has higher MAdds compared to MobileNetV2 [33], but it obtains 4.1% gain in top-1 accuracy with less number of parameters. Also, our EdgeNeXt-S outperforms ShuffleNetV2 [28] and MobileNetV3 [16] by 4.3% and 3.6% respectively, with comparable number of parameters.

**Comparison with ViTs.** Our EdgeNeXt outperforms recent ViT variants on ImageNet1K dataset with fewer parameters and MAdds. For example, EdgeNeXt-S obtains

78.8% top-1 accuracy, surpassing T2T-ViT [41] and DeiT-T [37] by 2.3% and 6.6% absolute margins respectively.

**Comparison with Hybrid Models.** EdgeNeXt outperforms MobileFormer [4], ViT-C [39], Coat-Lite-T [7] with less parameters and fewer MAdds (Table 2). For a fair comparison with MobileViT [29], we train our model at an input resolution of  $256 \times 256$  and show consistent gains for different models sizes (i.e., S, XS, and XXS) with fewer MAdds and faster inference on the edge devices (Table 3). For instance, our EdgeNeXt-XXS model achieves 71.2% top-1 accuracy with only 1.3M parameters, surpassing corresponding MobileViT model by 2.2%. Our EdgeNeXt-S model attains 79.4% accuracy on ImageNet with only 5.6M parameters, a margin of 1.0% as compared to the corresponding MobileViT-S model. This demonstrates the effectiveness and the generalization of our design.

### 4.4. Inference on Edge Devices

We compute the inference time of our EdgeNeXt models on the NVIDIA Jetson Nano edge device and compare it with the state-of-the-art MobileViT [29] model (Table 3). All the models are converted to TensorRT engines and inference is performed in FP16 mode. Our model attains low latency on the edge device with similar parameters, fewer MAdds, and higher top-1 accuracy. Table 3 also lists the inference time on A100 GPU for both MobileViT and EdgeNeXt models. It can be observed that our EdgeNeXt-XXS model is  $\sim 34\%$  faster than the MobileViT-XXS model on A100 as compared to only  $\sim 8\%$  faster on Jetson Nano, indicating that EdgeNeXt better utilizes the advanced hardware as compared to MobileViT.

### 4.5. Object Detection

We use EdgeNeXt as a backbone in SSDLite and finetune the model on COCO 2017 dataset [22] at an input resolution of  $320 \times 320$ . The difference between SSD [23] and SSDLite is that the standard convolutions are replaced with separable convolutions in the SSD head. The results are re-

<sup>1</sup><https://developer.nvidia.com/embedded/jetson-nano-developer-kit>

<sup>2</sup><https://github.com/NVIDIA/TensorRT>

Model	Date	Input	Params↓	MAdds↓	Top1↑	Jetson↓	A100↓
MobileViT-XXS			1.3M	364M	69.0	21.0 <i>ms</i>	216 $\mu$ s
MobileViT-XS	ICLR2022	256 <sup>2</sup>	2.3M	886M	74.8	35.1 <i>ms</i>	423 $\mu$ s
MobileViT-S			5.6M	2.01G	78.4	53.0 <i>ms</i>	559 $\mu$ s
EdgeNeXt-XXS			1.3M	261M	71.2	19.3 <i>ms</i>	142 $\mu$ s
EdgeNeXt-XS	Ours	256 <sup>2</sup>	2.3M	538M	75.0	31.6 <i>ms</i>	227 $\mu$ s
EdgeNeXt-S			5.6M	1.30G	79.4	48.8 <i>ms</i>	332 $\mu$ s

Table 3. Comparison of different variants of EdgeNeXt with the counterpart models of MobileViT. The last two columns list the latency in *ms* and  $\mu$ s on Jetson Nano and A100 devices, respectively. Our EdgeNext models provide higher accuracy with lower latency for each model size.

ported in Table 4. EdgeNeXt consistently outperforms MobileNet backbones and gives competitive performance compared to MobileViT backbone. With  $\sim 38\%$  fewer MAdds and comparable parameters, EdgeNeXt achieves 27.9 box AP which is 0.2 points more than MobileViT.

Model	Params↓	MAdds↓	mAP↑
MobileNetV1	5.1M	1.3G	22.2
MobileNetV2	4.3M	800M	22.1
MobileNetV3	5.0M	620M	22.0
MobileViT-S	5.7M	3.4G	27.7
EdgeNeXt-S (ours)	6.2M	2.1G	27.9

Table 4. Comparisons with SOTA on COCO object detection. EdgeNeXt improves over previous approaches.

#### 4.6. Semantic Segmentation

We use EdgeNeXt as backbone in DeepLabv3 [3] and finetune the model on Pascal VOC [10] dataset at an input resolution of  $512 \times 512$ . DeepLabv3 uses dilated convolution in cascade design along with spatial pyramid pooling to encode multi-scale features which are useful in encoding objects at multiple scales. Our model obtains 80.2 mIOU on the validation dataset, providing a 1.1 points gain over MobileViT with  $\sim 36\%$  fewer MAdds.

Model	Params↓	MAdds↓	mIOU↑
MobileNetV1	11.1M	14.2G	75.3
MobileNetV2	4.5M	5.8G	75.7
MobileViT-S	5.7M	13.7G	79.1
EdgeNeXt-S (ours)	6.5M	8.7G	80.2

Table 5. Comparisons with SOTA on VOC semantic segmentation. Our model provides reasonable gain over previous approaches.

### 5. Ablations

In this section, we ablate different design choices in our proposed EdgeNeXt model.

**SDTA encoder and adaptive kernel sizes.** Table 6 shows the importance of SDTA encoders and adaptive kernel sizes in our proposed architecture. Replacing SDTA encoders

with convolution encoders degrades the accuracy by 1.1%, indicating its usefulness in our design. When we fix kernel size to 7 in all four stages of the network, it further reduces the accuracy by 0.4%. Overall, our proposed design provides an optimal speed-accuracy trade-off.

We also ablate the contributions of SDTA components (e.g., adaptive branching and positional encoding) in Table 6. Removing adaptive branching and positional encoding slightly decreases the accuracy.

	Model	Top1↑	Latency↓
Base	EdgeNeXt-S	79.4	332 $\mu$ s
Different Components	w/o SDTA Encoders	78.3	265 $\mu$ s
	+ w/o Adaptive Kernels	77.9	301 $\mu$ s
SDTA Components	w/o Adaptive Branching	79.3	332 $\mu$ s
	+ w/o PE	79.2	301 $\mu$ s

Table 6. Ablation on different components of EdgeNeXt and SDTA encoder design. The results show the benefits of SDTA encoders and adaptive kernels in our design. Further, adaptive branching and positional encoding (PE) in our SDTA module are required to get the good accuracy.

**Hybrid design.** Table 7 ablates the different hybrid design choices for our EdgeNeXt model. Motivated from MetaFormer [40], we replace all convolutional modules in the last two stages with SDTA encoders. The results show superior performance when all blocks in the last two stages are SDTA blocks, but it increases the latency (row-2 vs 3). Our hybrid design where we propose to use an SDTA module as the last block in the last three stages provides an optimal speed-accuracy trade-off.

Model Configuration	Top1↑	Latency↓
1: Conv=[3, 3, 9, 0], SDTA=[0, 0, 0, 3]	79.3	303 $\mu$ s
2: Conv=[3, 3, 0, 0], SDTA=[0, 0, 9, 3]	79.7	393 $\mu$ s
3: Conv=[3, 2, 8, 2], SDTA=[0, 1, 1, 1]	79.4	332 $\mu$ s

Table 7. Ablation on the hybrid architecture of Conv. and SDTA encoders. Using one SDTA encoder as the last block in the last three stages provides an optimal accuracy-latency trade-off.

Table 8 provides an ablation of the importance of using SDTA encoders at different stages of the network. It is noticeable that progressively adding an SDTA encoder as the last

block of the last three stages improves the accuracy with some loss in inference latency. However, in row 4, we obtain the best trade-off between accuracy and speed where the SDTA encoder is added as the last block in the last three stages of the network. Further, we notice that adding a global SDTA encoder to the first stage of the network is not helpful where the features are not much mature.

Model Configuration	Top1↑	Latency↓
1: Conv=[3, 3, 9, 3], SDTA=[0, 0, 0, 0]	78.3	265 $\mu$ s
2: Conv=[3, 3, 9, 2], SDTA=[0, 0, 0, 1]	78.6	290 $\mu$ s
3: Conv=[3, 3, 8, 2], SDTA=[0, 0, 1, 1]	79.1	310 $\mu$ s
4: Conv=[3, 2, 8, 2], SDTA=[0, 1, 1, 1]	79.4	332 $\mu$ s
5: Conv=[2, 2, 8, 2], SDTA=[1, 1, 1, 1]	79.2	387 $\mu$ s

Table 8. Ablation on using SDTA encoder at different stages of the network. Including SDTA encoders in the last three stages improves performance, whereas a global SDTA encoder is not helpful in the first stage of the network.

We also provide an ablation on using the SDTA module at the start of each stage versus at the end of each stage. Table 9 shows that using the global SDTA encoder at the end of each stage is more beneficial. This observation is consistent with the recent work [21].

SDTA Configuration	Top1↑	Latency↓
Start of Stage (SDTA=[0, 1, 1, 1])	79.0	332 $\mu$ s
End of Stage (SDTA=[0, 1, 1, 1])	79.4	332 $\mu$ s

Table 9. Ablation on using SDTA at the start and end of each stage in EdgeNeXt. The results show that it is generally beneficial to use SDTA at the end of each stage.

**Activation and normalization.** EdgeNeXt uses GELU activation and layer normalization throughout the network. We found that the current PyTorch implementations of GELU and layer normalization are not optimal for high speed inference. To this end, we replace GELU with Hard-Swish and layer-norm with batch-norm and retrain our models. Fig. 3 indicates that it reduces the accuracy slightly, however, reduces the latency by a large margin.

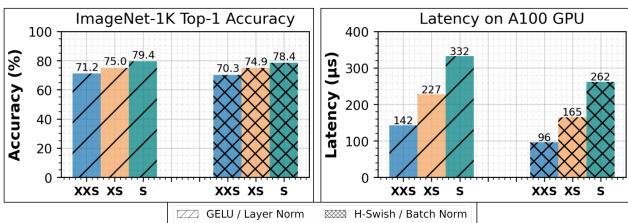


Figure 3. Ablation on the affect of using different activation functions and normalization layers on accuracy and latency of our network variants. Using Hard Swish activation and batch normalization instead of GELU and layer normalization significantly improves the latency at the cost of some loss in accuracy.

## 6. Qualitative Results

Figs. 4 and 5 show the qualitative results of EdgeNeXt-S detection and segmentation models respectively. Our model can precisely detect and segments objects in various views.

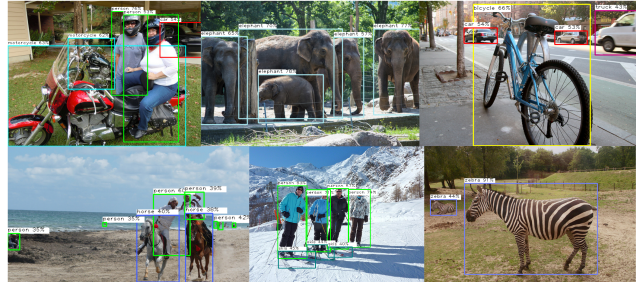


Figure 4. Qualitative results of our EdgeNeXt detection model on COCO validation dataset. The model is trained on COCO dataset with 80 detection classes. Our model can effectively localize and classify objects in diverse scenes.

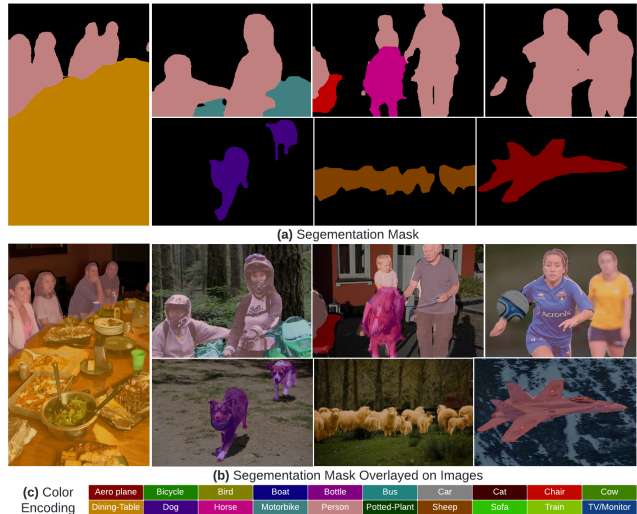


Figure 5. Qualitative results of EdgeNeXt-S segmentation model on unseen COCO validation dataset. The model is trained on VOC dataset with 20 segmentation classes. (a) shows the predicted semantic segmentation mask where ‘black ’color represents the background pixels. (b) displays the predicted masks on top of original images. (c) represents the color encodings for all VOC classes for the displayed segmentation masks. Our model provides high-quality segmentation masks on unseen COCO images.

## 7. Conclusion

The success of the transformer models comes with a higher computational overhead compared to CNNs. Self-attention operation is the major contributor to this overhead, which makes vision transformers slow on the edge devices compared to CNN-based mobile architectures. In this paper, we introduce a hybrid design consisting of convolution and efficient self-attention based encoders to jointly model

local and global information effectively, while being efficient in terms of both parameters and MAdds on vision tasks with superior performance compared to state-of-the-art methods. Our experimental results show promising performance for different variants of EdgeNeXt, which demonstrates the effectiveness and the generalization ability of the proposed model.

## References

- [1] Alaaeldin Ali, Hugo Touvron, Mathilde Caron, Piotr Bojanowski, Matthijs Douze, Armand Joulin, Ivan Laptev, Natalia Neverova, Gabriel Synnaeve, Jakob Verbeek, et al. Xcit: Cross-covariance image transformers. *Advances in Neural Information Processing Systems*, 2021. 4
- [2] Jimmy Lei Ba, Jamie Ryan Kiros, and Geoffrey E Hinton. Layer normalization. *arXiv preprint arXiv:1607.06450*, 2016. 3
- [3] Liang-Chieh Chen, George Papandreou, Florian Schroff, and Hartwig Adam. Rethinking atrous convolution for semantic image segmentation. *arXiv preprint arXiv:1706.05587*, 2017. 7
- [4] Yinpeng Chen, Xiyang Dai, Dongdong Chen, Mengchen Liu, Xiaoyi Dong, Lu Yuan, and Zicheng Liu. Mobileformer: Bridging mobilenet and transformer. In *Proceedings of the IEEE/CVF Conference on Computer Vision and Pattern Recognition*, 2022. 2, 6
- [5] François Chollet. Xception: Deep learning with depthwise separable convolutions. In *Proceedings of the IEEE/CVF Conference on Computer Vision and Pattern Recognition*, 2017. 2
- [6] Ekin Dogus Cubuk, Barret Zoph, Jon Shlens, and Quoc Le. Randaugment: Practical automated data augmentation with a reduced search space. In *Advances in Neural Information Processing Systems*, 2020. 5
- [7] Zihang Dai, Hanxiao Liu, Quoc Le, and Mingxing Tan. Coatnet: Marrying convolution and attention for all data sizes. *Advances in Neural Information Processing Systems*, 2021. 6
- [8] Alexey Dosovitskiy, Lucas Beyer, Alexander Kolesnikov, Dirk Weissenborn, Xiaohua Zhai, Thomas Unterthiner, Mostafa Dehghani, Matthias Minderer, Georg Heigold, Sylvain Gelly, et al. An image is worth 16x16 words: Transformers for image recognition at scale. *arXiv preprint arXiv:2010.11929*, 2020. 2
- [9] Stéphane d’Ascoli, Hugo Touvron, Matthew L Leavitt, Ari S Morcos, Giulio Biroli, and Levent Sagun. Convit: Improving vision transformers with soft convolutional inductive biases. In *International Conference on Machine Learning*, 2021. 2
- [10] Mark Everingham, Luc Van Gool, Christopher KI Williams, John Winn, and Andrew Zisserman. The Pascal Visual Object Classes (VOC) Challenge. *International Journal of Computer Vision*, 88(2):303–338, 2010. 5, 7
- [11] Haoqi Fan, Bo Xiong, Karttikeya Mangalam, Yanghao Li, Zhicheng Yan, Jitendra Malik, and Christoph Feichtenhofer. Multiscale vision transformers. In *Proceedings of the IEEE/CVF International Conference on Computer Vision*, 2021. 2
- [12] Shang-Hua Gao, Ming-Ming Cheng, Kai Zhao, Xin-Yu Zhang, Ming-Hsuan Yang, and Philip Torr. Res2net: A new multi-scale backbone architecture. *IEEE Transactions on Pattern Analysis and Machine Intelligence*, 43(2):652–662, 2019. 4
- [13] Bharath Hariharan, Pablo Arbeláez, Lubomir Bourdev, Subhransu Maji, and Jitendra Malik. Semantic contours from inverse detectors. In *Proceedings of the IEEE/CVF International Conference on Computer Vision*, 2011. 5
- [14] Kaiming He, Xiangyu Zhang, Shaoqing Ren, and Jian Sun. Deep residual learning for image recognition. In *Proceedings of the IEEE/CVF Conference on Computer Vision and Pattern Recognition*, 2016. 3
- [15] Dan Hendrycks and Kevin Gimpel. Gaussian error linear units (gelus). *arXiv preprint arXiv:1606.08415*, 2016. 3
- [16] Andrew Howard, Mark Sandler, Grace Chu, Liang-Chieh Chen, Bo Chen, Mingxing Tan, Weijun Wang, Yukun Zhu, Ruoming Pang, Vijay Vasudevan, et al. Searching for mobilenetv3. In *Proceedings of the IEEE/CVF International Conference on Computer Vision*, 2019. 1, 2, 6
- [17] Andrew G. Howard, Menglong Zhu, Bo Chen, Dmitry Kalenichenko, Weijun Wang, Tobias Weyand, Marco Andreetto, and Hartwig Adam. Mobilenets: Efficient convolutional neural networks for mobile vision applications. *CoRR*, abs/1704.04861, 2017. 2, 5
- [18] Gao Huang, Yu Sun, Zhuang Liu, Daniel Sedra, and Kilian Q Weinberger. Deep networks with stochastic depth. In *The European Conference on Computer Vision*, 2016. 5
- [19] Forrest N Iandola, Song Han, Matthew W Moskewicz, Khalid Ashraf, William J Dally, and Kurt Keutzer. Squeezenet: Alexnet-level accuracy with 50x fewer parameters and 0.5 mb model size. *arXiv preprint arXiv:1602.07360*, 2016. 1, 2
- [20] Salman Khan, Muzammal Naseer, Munawar Hayat, Syed Waqas Zamir, Fahad Shahbaz Khan, and Mubarak Shah. Transformers in vision: A survey. *ACM Computing Surveys (CSUR)*, 2021. 1
- [21] Yanghao Li, Chao-Yuan Wu, Haoqi Fan, Karttikeya Mangalam, Bo Xiong, Jitendra Malik, and Christoph Feichtenhofer. Improved multiscale vision transformers for classification and detection. In *Proceedings of the IEEE/CVF Conference on Computer Vision and Pattern Recognition*, 2022. 8
- [22] Tsung-Yi Lin, Michael Maire, Serge Belongie, James Hays, Pietro Perona, Deva Ramanan, Piotr Dollár, and C Lawrence Zitnick. Microsoft coco: Common objects in context. In *The European Conference on Computer Vision*, 2014. 5, 6
- [23] Wei Liu, Dragomir Anguelov, Dumitru Erhan, Christian Szegedy, Scott Reed, Cheng-Yang Fu, and Alexander C Berg. Ssd: Single shot multibox detector. In *The European Conference on Computer Vision*, 2016. 6
- [24] Ze Liu, Yutong Lin, Yue Cao, Han Hu, Yixuan Wei, Zheng Zhang, Stephen Lin, and Baining Guo. Swin transformer: Hierarchical vision transformer using shifted windows. In *Proceedings of the IEEE/CVF International Conference on Computer Vision*, 2021. 2
- [25] Zhuang Liu, Hanzi Mao, Chao-Yuan Wu, Christoph Feichtenhofer, Trevor Darrell, and Saining Xie. A convnet for the

- 2020s. In *Proceedings of the IEEE/CVF Conference on Computer Vision and Pattern Recognition*, 2022. 3, 6
- [26] Ilya Loshchilov and Frank Hutter. Sgdr: Stochastic gradient descent with warm restarts. In *International Conference on Learning Representations*, 2017. 5
- [27] Ilya Loshchilov and Frank Hutter. Decoupled weight decay regularization. In *International Conference on Learning Representations*, 2019. 5
- [28] Ningning Ma, Xiangyu Zhang, Hai-Tao Zheng, and Jian Sun. Shufflenet v2: Practical guidelines for efficient cnn architecture design. In *The European Conference on Computer Vision*, 2018. 1, 6
- [29] Sachin Mehta and Mohammad Rastegari. Mobilevit: light-weight, general-purpose, and mobile-friendly vision transformer. In *International Conference on Learning Representations*, 2022. 2, 3, 5, 6
- [30] Sachin Mehta, Mohammad Rastegari, Linda Shapiro, and Hannaneh Hajishirzi. Espnetv2: A light-weight, power efficient, and general purpose convolutional neural network. In *Proceedings of the IEEE/CVF Conference on Computer Vision and Pattern Recognition*, 2019. 2
- [31] Boris T Polyak and Anatoli B Juditsky. Acceleration of stochastic approximation by averaging. *SIAM journal on control and optimization*, 1992. 5
- [32] Olga Russakovsky, Jia Deng, Hao Su, Jonathan Krause, Sanjeev Satheesh, Sean Ma, Zhiheng Huang, Andrej Karpathy, Aditya Khosla, Michael Bernstein, et al. ImageNet Large Scale Visual Recognition Challenge. *International Journal of Computer Vision*, 115(3):211–252, 2015. 2, 5
- [33] Mark Sandler, Andrew Howard, Menglong Zhu, Andrey Zhmoginov, and Liang-Chieh Chen. Mobilenetv2: Inverted residuals and linear bottlenecks. In *Proceedings of the IEEE/CVF Conference on Computer Vision and Pattern Recognition*, 2018. 1, 2, 6
- [34] Jürgen Schmidhuber. Deep learning in neural networks: An overview. *Neural networks*, 61:85–117, 2015. 1
- [35] Aravind Srinivas, Tsung-Yi Lin, Niki Parmar, Jonathon Shlens, Pieter Abbeel, and Ashish Vaswani. Bottleneck transformers for visual recognition. In *Proceedings of the IEEE/CVF Conference on Computer Vision and Pattern Recognition*, 2021. 2
- [36] Mingxing Tan, Bo Chen, Ruoming Pang, Vijay Vasudevan, Mark Sandler, Andrew Howard, and Quoc V Le. Mnasnet: Platform-aware neural architecture search for mobile. In *Proceedings of the IEEE/CVF Conference on Computer Vision and Pattern Recognition*, 2019. 1, 2
- [37] Hugo Touvron, Matthieu Cord, Matthijs Douze, Francisco Massa, Alexandre Sablayrolles, and Hervé Jégou. Training data-efficient image transformers & distillation through attention. In *International Conference on Machine Learning*, 2021. 2, 6
- [38] Ashish Vaswani, Noam Shazeer, Niki Parmar, Jakob Uszkoreit, Llion Jones, Aidan N Gomez, Łukasz Kaiser, and Illia Polosukhin. Attention is all you need. In *Advances in Neural Information Processing Systems*, 2017. 2
- [39] Tete Xiao, Piotr Dollar, Mannat Singh, Eric Mintun, Trevor Darrell, and Ross Girshick. Early convolutions help transformers see better. In *Advances in Neural Information Processing Systems*, 2021. 2, 6
- [40] Weihao Yu, Mi Luo, Pan Zhou, Chenyang Si, Yichen Zhou, Xinchao Wang, Jiashi Feng, and Shuicheng Yan. Metaformer is actually what you need for vision. In *Proceedings of the IEEE/CVF Conference on Computer Vision and Pattern Recognition*, 2021. 7
- [41] Li Yuan, Yunpeng Chen, Tao Wang, Weihao Yu, Yujun Shi, Zi-Hang Jiang, Francis EH Tay, Jiashi Feng, and Shuicheng Yan. Tokens-to-token vit: Training vision transformers from scratch on imagenet. In *Proceedings of the IEEE/CVF International Conference on Computer Vision*, 2021. 6
- [42] Matthew D Zeiler and Rob Fergus. Visualizing and understanding convolutional networks. In *The European Conference on Computer Vision*, 2014. 3
- [43] Haokui Zhang, Wenze Hu, and Xiaoyu Wang. Edgeformer: Improving light-weight convnets by learning from vision transformers. *arXiv preprint arXiv:2203.03952*, 2022. 2
- [44] Xiangyu Zhang, Xinyu Zhou, Mengxiao Lin, and Jian Sun. Shufflenet: An extremely efficient convolutional neural network for mobile devices. In *Proceedings of the IEEE/CVF Conference on Computer Vision and Pattern Recognition*, 2018. 2
- [45] Jingkai Zhou, Pichao Wang, Fan Wang, Qiong Liu, Hao Li, and Rong Jin. Elsa: Enhanced local self-attention for vision transformer. *arXiv preprint arXiv:2112.12786*, 2021. 2